Smith, A. *et al.* (2014) ***Géotechnique Letters*** **4**, 255–261, http://dx.doi.org/10.1680/geolett.14.00053

Acoustic emission monitoring of a soil slope: Comparisons with continuous deformation measurements

A. SMITH*, N. DIXON*, P. MELDRUM†, E. HASLAM† and J. CHAMBERS†

Acoustic emission (AE) has become an established approach to monitor the stability of soil slopes. However, the challenge has been to develop strategies to interpret and quantify deformation behaviour from the measured AE. This paper presents the first comparison of continuous AE (measured using an active waveguide) and continuous subsurface deformation measurements. The active waveguide is installed in a borehole through a slope and comprises a metal waveguide rod or tube with a granular backfill surround. When the host slope deforms, the column of granular backfill also deforms, generating AE that can propagate along the waveguide. This paper presents results from a field trial at a reactivated soil slope in North Yorkshire, UK. The measurements confirm that AE rates generated are directly proportional to the velocity of slope movement (e.g. the AE rate versus velocity relationship determined for a series of slope movement events produced an R^2 value of 0·8) and demonstrate the performance of AE monitoring of active waveguides to provide continuous information on slope displacements and displacement rates with high temporal resolution.

KEYWORDS: deformation; field instrumentation; landslides; slopes

INTRODUCTION AND BACKGROUND

In soil, acoustic emission (AE) is generated by inter-particle friction and hence the detection of AE is an indication of deformation. The dominant mechanisms for AE generation within soil are particle–particle interactions such as sliding and rolling friction, particle contact network rearrangement (e.g. release of contact stress and stress redistribution as interlock is overcome and regained) and degradation at particle asperities where contact stresses are very high (Lord & Koerner, 1974; Michlmayr *et al.*, 2012a, 2012b, 2013). Research contributions (Koerner *et al.*, 1981; Mitchell & Romeril, 1984; Garga & Chichibu, 1990; Shiotani & Ohtsu, 1999; Michlmayr *et al.*, 2013) in understanding the fundamental AE behaviour of soil have demonstrated that

- deforming soil produces detectable AE
- the characteristics of AE generated are governed by the properties of the soil (e.g. AE from fine-grained soils is highly influenced by moisture content and plasticity, and AE events with greater magnitude are produced in granular soil with large angular particles)
- the magnitude of AE generated is directly related to the stress state of the soil (e.g. AE events with greater magnitude are generated by deforming soil with high inter-particle contact stresses).

Various authors have used AE monitoring to assess the stability of both natural and constructed slopes (e.g. Beard, 1961; Cadman & Goodman, 1967; Chichibu *et al.*, 1989; Naemura *et al.*, 1990; Nakajima *et al.*, 1991; Rouse *et al.*, 1991; Fujiwara *et al.*, 1999; Dixon *et al.*, 2003, 2014). Fine-grained soils generate relatively low energy AE signals and these attenuate significantly over short distances. In order to monitor AE generated by deforming slopes formed of fine-grained soils, Dixon *et al.* (2003) devised the active waveguide. The active waveguide (shown in Fig. 1) is installed in a borehole that penetrates any shear surface or potential shear surface beneath the slope; it comprises a steel waveguide (to transport the AE signals generated at the shear surface to the ground surface with relatively low attenuation) and angular gravel backfill (to generate relatively high energy AE as the slope deforms, which can propagate along the waveguide). Field trials conducted by Dixon *et al.* (2003) proved that AE monitoring of active waveguides has the potential to detect pre-failure deformations earlier than conventional inclinometers, and that active waveguides continue to generate AE beyond deformation magnitudes sufficient to shear off inclinometer casings and render them unusable. Dixon & Spriggs (2007) demonstrated that an increase in the applied deformation rate to active waveguide models resulted in a proportional increase in the AE rates generated; AE rates are typically defined as the number of times the amplitude of the wave crosses a pre-defined voltage threshold per unit time (i.e. ring-down counts (RDC) as shown in Fig. 2). AE monitoring using active waveguides is most applicable to soil slopes that fail along a defined shear surface as the development of such a surface, or reactivation of an existing surface, will shear the waveguide granular backfill and generate high levels of detectable AE.

Dixon *et al.* (2014) introduced a coefficient of proportionality, C_p, as a function that defines the empirical relationship between AE rates generated from the active waveguide system in response to an applied velocity of slope movement

$$\begin{aligned} &\mathrm{AE}_{\mathrm{rate}} \propto \mathrm{Velocity} \\ &\therefore \mathrm{AE}_{\mathrm{rate}} = C_p \times \mathrm{Velocity} \end{aligned} \quad (1)$$

where $C_p = f(\text{variables})$.

An increasing rate of deformation (i.e. in response to increasing slope velocity) within the active waveguide

Manuscript received 16 July 2014; first decision 20 August 2014; accepted 5 September 2014.
Published online at www.geotechniqueletters.com on 6 October 2014.
*School of Civil and Building Engineering, Loughborough University, Loughborough, UK
†British Geological Survey, Keyworth, UK

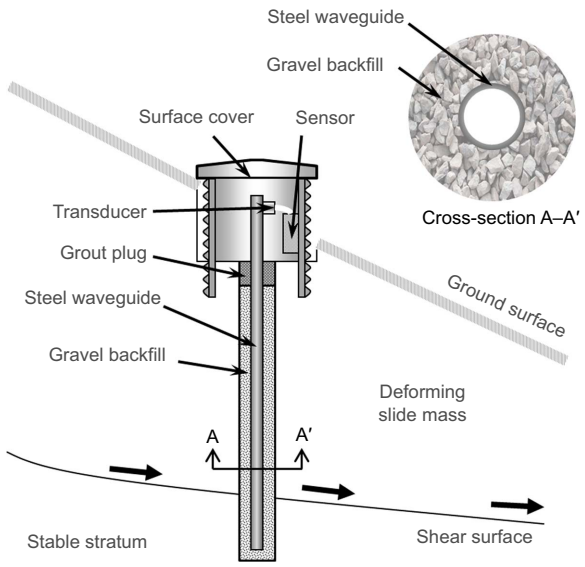

Fig. 1. Schematic illustration of an active waveguide installed through a slope with an ALARMS sensor connected at the ground surface (after Dixon *et al.* (2012))

generates an increasing number of particle–particle/particle–waveguide interactions. Each of these interactions generates a transient AE event. These transient AE events combine and propagate along the waveguide where they are monitored by a sensor at the ground surface. Hence, AE rates produced and measured by the system are proportional to the velocity of slope movement. The coefficient of proportionality is a measure of the system's sensitivity (i.e. the magnitude of AE rates produced in response to an applied velocity) and is dependent on many variables related to the AE measurement system, such as

- the sensor sensitivity, which is controlled by signal amplification and voltage threshold level
- the depth to the shear surface, which influences the magnitude of AE signal attenuation as it is transmitted from the shear zone to the ground surface by the waveguide
- active waveguide properties such as the tube geometry and backfill properties.

The magnitude of AE rate responses produced by each measurement system will depend on these factors, in addition to the rate of slope displacement. As the measured AE is generated by deformation of the active waveguide and not the host soil slope, a standard active waveguide design allows application of a generic AE rate–slope velocity relationship independent of the properties of the host soil slope.

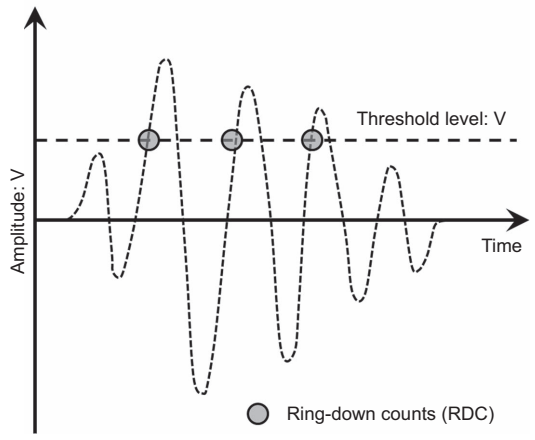

Fig. 2. Simplified AE waveform with voltage threshold crossings (ring-down counts) identified

Dixon *et al.* (2014) report monitoring of a reactivated soil slope using active waveguides and demonstrate how the coefficient of proportionality, if the AE rate–velocity relationship is assumed to be linear, can be back-calculated from slide events. AE rates are the derivative of AE energy (i.e. cumulative RDC) with respect to time, and velocity is the derivative of displacement with respect to time. Therefore, using the shape of the AE rate–time profile, it was possible to determine a velocity–time profile for a slope movement event by equating the area under the AE rate–time curve to the magnitude of displacement measured by an adjacent inclinometer. The total event displacement was distributed proportionately to each trapezoidal integrand under the curve and the velocity over each trapezoid was determined using the displacement–time relation. Each point in time throughout the event subsequently had an AE rate and a corresponding velocity, and therefore a linear AE rate–velocity calibration could be determined. This allowed the velocity and cumulative displacement in subsequent slope deformation events to be quantified by applying the coefficient of proportionality to measured AE rates; an example is shown in Fig. 3. This method was shown to generate errors significantly less than an order of magnitude and is therefore consistent with standard classification for landslide movements (e.g. Schuster & Krizek, 1978; Cruden & Varnes, 1996; Anderson & Holcombe, 2013: p. 92).

This paper presents a comparison of continuous AE measurements, detected from an active waveguide installed at the same reactivated landslide as reported in Dixon *et al.* (2014), with continuous subsurface deformation measurements provided by an adjacent ShapeAccelArray (SAA). The SAA comprises a string of MEMS (micro-electro-mechanical systems) sensors installed at regular intervals along the depth of a borehole; each sensor can monitor three-dimensional displacements accurately, continuously and with high temporal resolution. This is the first study that has allowed comparison of continuous AE and continuous deformation measurements (previous studies have made comparisons using manually read inclinometers at intervals and therefore with low temporal resolution). The Slope ALARMS AE measurement system (Dixon & Spriggs, 2011) employed in the study (Fig. 1) was the same as that used by Dixon *et al.* (2014). A 30 kHz resonant frequency transducer was coupled to the waveguide at the ground surface to convert the AE into voltages; the electrical signal was subsequently processed (i.e. amplified and filtered to keep only signals with frequencies in the range 20–30 kHz as this removed low-frequency environmental noise) and RDC were recorded and time stamped for pre-determined time intervals (30 min intervals were used in this study), continuously and in real-time.

THE HOLLIN HILL CASE STUDY

Introduction

Hollin Hill is a complex of interacting landslides situated 11 km to the west of Malton, North Yorkshire, UK (latitude 54·111044, longitude −0·95948786). The landslides at Hollin Hill can be characterised as shallow rotational failures at the top of the slope that feed into larger-scale slowly moving lobes of slumped material; the rotational features and active lobes extend approximately 150 m down the slope from the top of the hill. Movement typically occurs in the winter months (i.e. January and February) when the

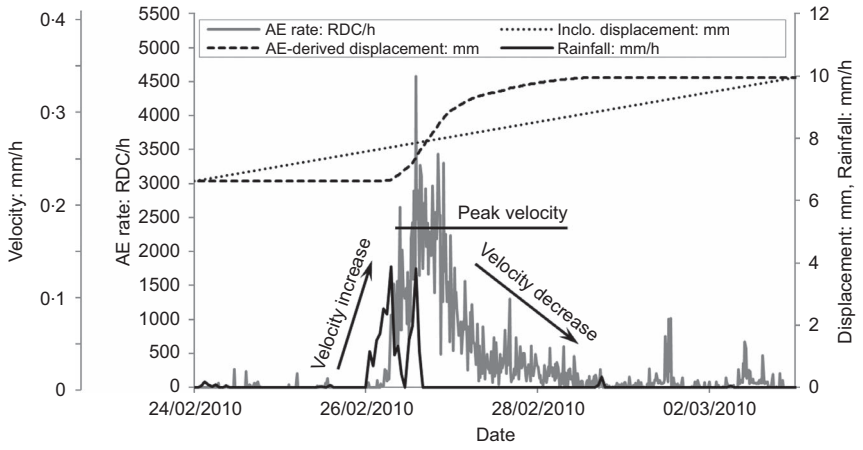

Fig. 3. AE rate, AE derived velocity, inclinometer-measured displacement, AE-derived displacement and rainfall time series for a reactivated slope deformation event at cluster 2 at Hollin Hill (after Dixon *et al.* (2014))

slope is at its wettest. The consistent occurrence of reactivated slide events and its remote location in farmland (i.e. having no threat to infrastructure) make Hollin Hill an ideal site to trial new landslide monitoring techniques; the British Geological Survey has investigated and monitored landslides at Hollin Hill for several years (e.g. Chambers *et al.*, 2008, 2011; Gunn *et al.*, 2013; Merritt *et al.*, 2013). Two of the lobes of slumped material were instrumented with three clusters of active waveguides (as described by Dixon *et al.* (2014)); the instrumentation cluster locations are shown in Fig. 4(a). This paper reports measurements recorded by an active waveguide (AEWG3) and SAA (SAA3) installed at cluster 3 on the eastern lobe in Fig. 4(a). A cross-section taken through the eastern lobe at instrumentation cluster 3 is shown in Fig. 4(b).

AEWG3 was installed in a 130 mm diameter borehole to 5·7 m below ground level. The waveguide comprised two 3 m lengths of 50 mm diameter 3 mm thick steel tubing connected with screw-threaded couplings. The annulus around the waveguide was backfilled with angular 5–10 mm gravel compacted in nominally 0·25 m high lifts. The top 0·3 m of the borehole was backfilled with a bentonite grout plug to seal against the ingress of surface water. The steel tube protruded 0·3 m above ground level, where the transducer was coupled, and was encased in a secure protective chamber (as shown in Fig. 1). SAA3 was installed 1 m west of AEWG3 to a depth of 2·5 m.

Comparison of continuous AE and continuous deformation measurements

A series of reactivated slope movements (i.e. small-magnitude displacements with low velocities as the shear surface is already at or near residual strength (Hutchinson, 1988; Leroueil, 2001)) occurred in response to periods of rainfall that produced transient elevations in pore-water pressure along the shallow shear surface in January 2014. Figure 5 shows the resultant horizontal displacement and velocity time series measured from 0·3 m depth in SAA3 (day 0 was 9 January 2014). Each of the slide events was

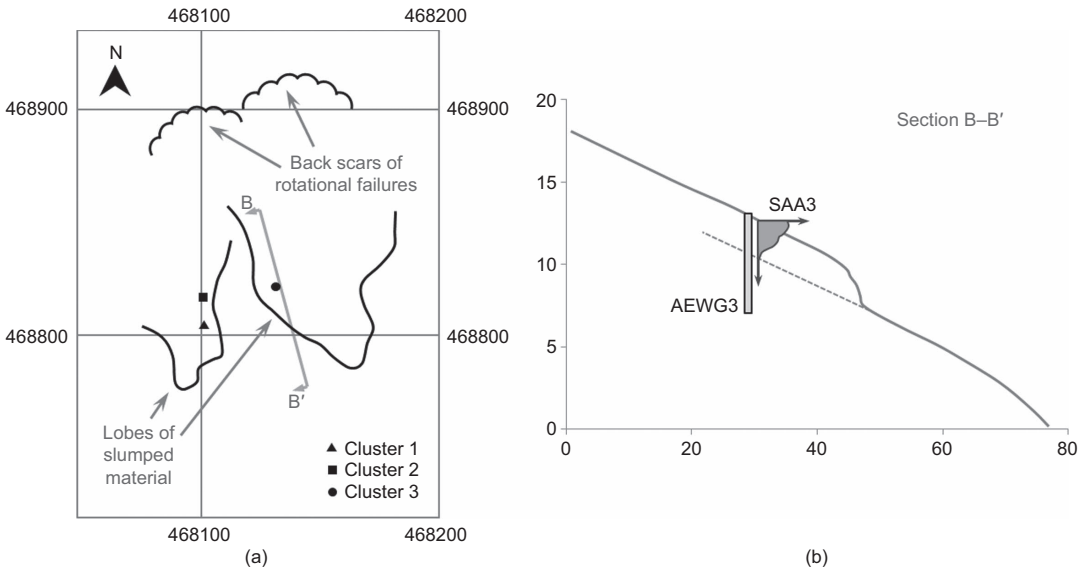

Fig. 4. Hollin Hill landslide: (a) site plan with instrumentation clusters highlighted (UK Ordnance Survey grid reference system); (b) cross-section through the eastern lobe at instrumentation cluster 3 with exaggerated SAA3 data showing the depth to the shear surface (cross-section axes in metres)

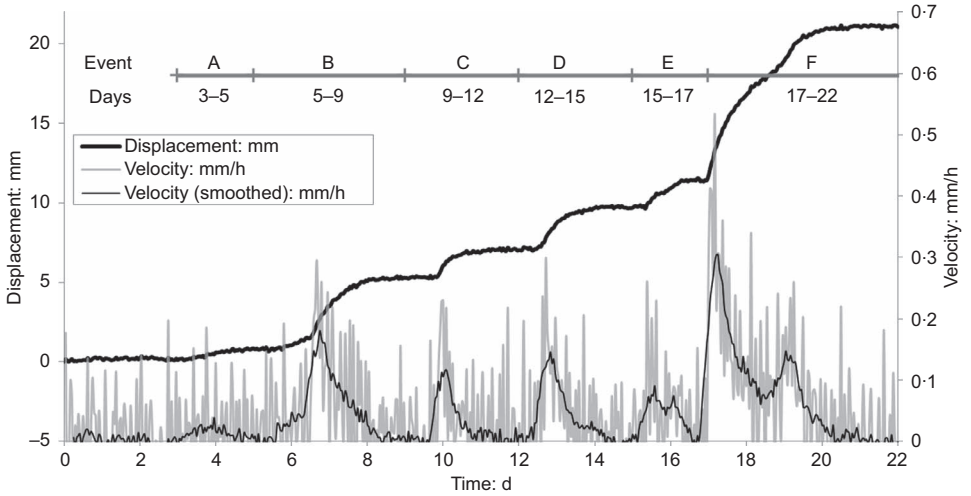

Fig. 5. Resultant displacement–time, velocity–time and smoothed velocity–time measured by SAA3 for a series of reactivated slide events at cluster 3

allocated an event identification (A to F). Figure 6 highlights the triggering rainfall preceding the slide events. The duration of the movement events varied between 3 and 6 d, with the peak velocity reaching approximately 0·35 mm/h in event F. The total displacement (resultant horizontal) measured over the period of 22 d at 0·3 m depth in SAA3 was approximately 22 mm. The displacement–depth profile recorded by SAA3 is shown in Fig. 7 with readings presented at the cessation of each event. It is clear that the main shear surface is at a depth between 1·5 and 2·0 m at the location of SAA3 and AEWG3.

In Fig. 5 the SAA-measured velocity–time data are superimposed with a smoother curve of ten-hour moving average (THMA) values; the THMA values were determined through calculation of the average of the velocity over the 5 h preceding and 5 h succeeding each measurement. THMA values were used for smoothing in order to reduce variability in the raw SAA data (60 min measurement intervals). The variability in the SAA measurements was of a similar magnitude as the slope movement velocities (i.e. $<0{\cdot}5$ mm/h); such variability would be less significant at greater velocities and therefore the need for smoothing would be reduced.

Figure 6 shows the cumulative RDC–time relationship recorded by the sensor coupled to AEWG3; the relationship is analogous to the cumulative displacement–time trend recorded by SAA3. Figure 8 shows the AE rate time series, also superimposed using a smoothed curve of THMA values (the sporadic nature of the raw data is due to slip–stick deformations taking place within the gravel backfill), which is analogous to the velocity–time profiles shown in Fig. 5. These comparisons confirm that

- AE rates generated by the system are directly proportional to the rate of deformation (i.e. slope velocity)
- AE monitoring of active waveguides using a sensor such as Slope ALARMS can provide continuous information on slope displacements and displacement rates
- the AE monitoring technique is sensitive to small displacements, displacement rates (i.e. <1 mm/h) and changes in displacement rates (i.e. accelerations and decelerations).

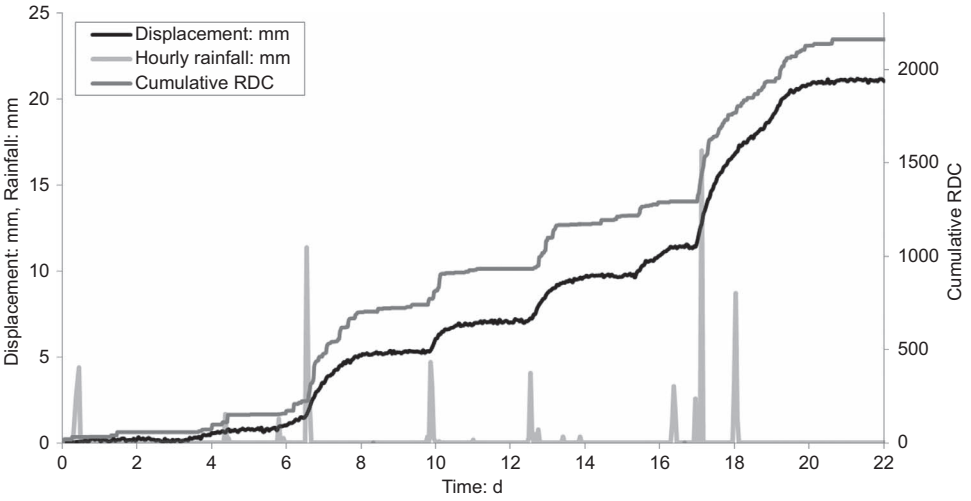

Fig. 6. Resultant measured displacement–time, cumulative RDC–time and hourly rainfall–time for the series of slide events at cluster 3

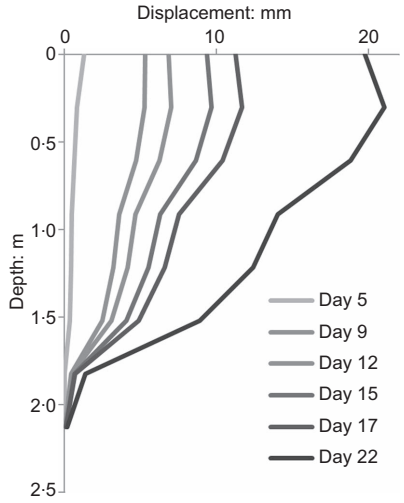

Fig. 7. Change in shape of SAA3 depth profile at the end of each slope displacement event at cluster 3

To define a measured relationship between AE rate and slope velocity from the continuous time series measurements, the THMA values of AE rates and measured slope velocity (i.e. Figs 5 and 8) were plotted (Fig. 9). Figure 9 shows, for the first time, an AE rate–velocity relationship derived from continuous time series measurements. A back-calculated relationship was subsequently determined using the method described by Dixon *et al.* (2014) and summarised in the introduction to this paper; this back-calculated linear relationship passes directly through the measured data points, as can be seen in Fig. 9. A linear regression line was calculated through all of the measured data points and, assuming it passed through the origin, it aligned almost exactly with the back-calculated relationship shown; the equation for the trend line is given in Fig. 9, which produced an R^2 value of 0·8. From the calibration in Fig. 9 it is now possible to derive slope displacement rates from measured AE rates generated from the system in response to subsequent slide events. Use of the back-calculation method to derive AE rate–velocity calibration relationships has therefore been shown to be an

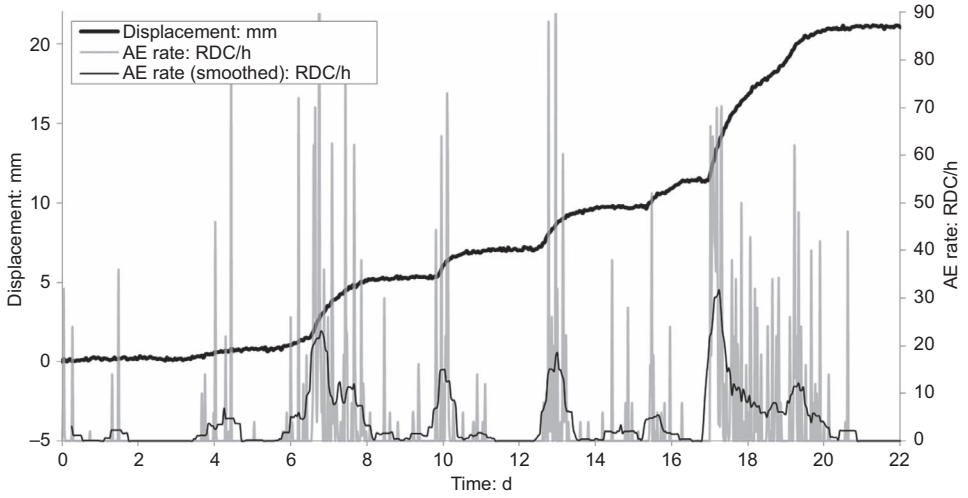

Fig. 8. Resultant measured displacement, AE rate and smoothed AE rate against time for the series of slide events at cluster 3

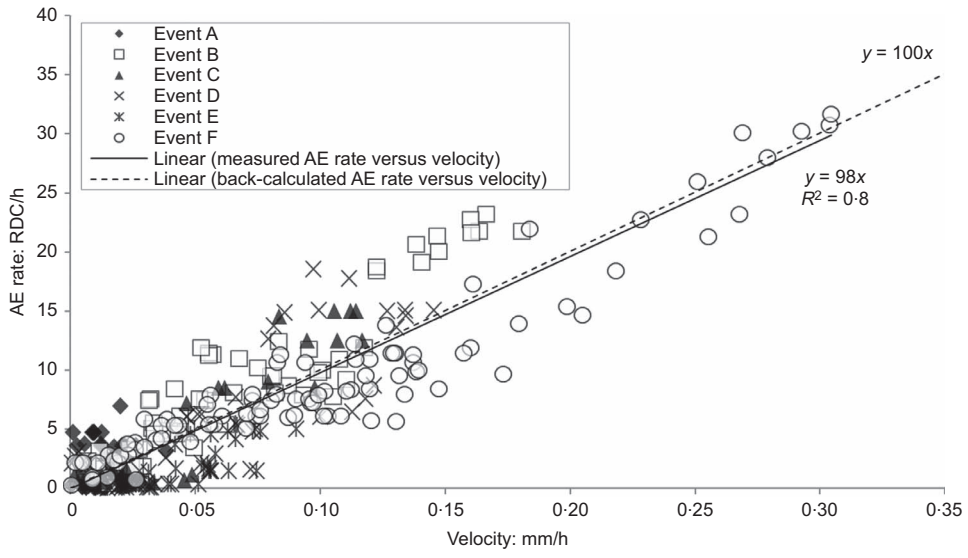

Fig. 9. Measured (THMA values taken from AEWG3 and SAA3 during slide events) and back-calculated AE rate–velocity relationships

appropriate technique for quantifying low-velocity (i.e. of the order of millimetres per hour or less) slope movements.

These field measurements have allowed the first comparison of continuous time series AE and slope displacement measurements to be made with relatively high temporal resolution. The study has established that the AE monitoring approach can be used to provide continuous information on slope displacements and displacement rates. It is anticipated that Slope ALARMS could provide this level of information at lower cost than other more commonly used real-time monitoring systems.

ADDITIONAL CONSIDERATIONS AND ONGOING RESEARCH

Laboratory experiments and field trials are ongoing in order to quantify the influence of variables (e.g. depth to shear surface and sensor sensitivity) on the coefficient of proportionality that defines the empirical AE rate–velocity relationship. Determination of a generic expression for the coefficient of proportionality will allow the Slope ALARMS monitoring approach to be utilised as a standalone technique without the need for use in combination with adjacent inclinometer/SAA systems for site-specific calibration. Additionally, the AE rate response from the system to first-time rupture landslide failure (as opposed to reactivation slide events, which have modest speed and travel), where the velocity progresses over several orders of magnitude, is also being investigated through laboratory experimentation and field trials.

SUMMARY

The paper summarises the use of active waveguides as subsurface instrumentation to monitor AE generated in response to slope movements and to assess the stability of soil slopes. The paper presented the first comparison of continuous AE (detected from an active waveguide) and continuous subsurface deformation measurements recorded using a ShapeAccelArray (SAA). The data were acquired from a field trial at a reactivated soil slope in North Yorkshire, UK. The results prove that AE rates generated are directly proportional to the velocity of slope movement. They also demonstrate the performance of AE monitoring of active waveguides to provide continuous information on slope displacements and displacement rates with high temporal resolution. Laboratory experiments and field trials are ongoing to establish

- a generic expression for the coefficient of proportionality, which defines the empirical AE rate–velocity relationship
- the AE rate response to first-time rupture failure, where the velocity of slope movement varies over several orders of magnitude.

ACKNOWLEDGEMENTS

The authors extend their sincerest gratitude to Steve and Josie Gibson (Hollin Hill landowners) for their support and cooperation in this research. P. Meldrum, E. Haslam and J. Chambers publish with the permission of the Executive Director of the British Geological Survey (NERC). The UK Engineering and Physical Sciences Research Council (EPSRC) funded much of the Slope ALARMS research and development. Thanks also go to Matthew Spriggs for his help in the early stages of the project.

REFERENCES

Anderson, M. G. & Holcombe, E. (2013). *Community-based landslide risk reduction: managing disasters in small steps*. Washington, DC: World Bank.

Beard, F. D. (1961). Predicting slides in cut slopes. *Western Construct San Francisco* **36**, 72.

Cadman, J. D. & Goodman, R. E. (1967). Landslide noise. *Science* **158**, No. 3805, 1182–1184.

Chambers, J. E., Weller, A. L., Gunn, D. A. *et al*. (2008). Geophysical anatomy of the Hollin Hill landslide, North Yorkshire, UK. *Proc. Near Surface 2008 – 14th European Meeting of Environmental and Engineering Geophysics, Krakow, Poland*, pp. 1–4.

Chambers, J. E., Wilkinson, P. B., Kuras, O. *et al*. (2011). Three-dimensional geophysical anatomy of an active landslide in Lias Group Mudrocks, Cleveland Basin, UK. *Geomorphology* **125**, No. 4, 472–484.

Chichibu, A., Jo, K., Nakamura, M., Goto, T. & Kamata, M. (1989). Acoustic emission characteristics of unstable slopes. *J. Acoust. Emiss*. **8**, No. 4, 107–112.

Cruden, D. & Varnes, D. J. (1996). Landslide types and processes. In *Landslides: Investigation and mitigation*. Washington, DC: Transportation Research Board, Publication 247, pp. 36–75.

Dixon, N. & Spriggs, M. (2007). Quantification of slope displacement rates using acoustic emission monitoring. *Can. Geotech. J*. **44**, No. 6, 966–976.

Dixon, N. & Spriggs, M. (2011). *Apparatus and method for monitoring soil slope displacement rate*. UK Patent GB 2467419A, May 2011.

Dixon, N., Hill, R. & Kavanagh, J. (2003). Acoustic emission monitoring of slope instability: development of an active wave guide system. *Proc. Inst. Civ. Eng. Geotech. Engng* **156**, No. 2, 83–95.

Dixon, N., Spriggs, M. P., Meldrum, P. & Haslam, E. (2012). Field trial of an acoustic emission early warning system for slope instability. In *Landslides and engineered slopes: Protecting society through improved understanding*. Banff, Alberta, Canada: CRC Press, pp. 1399–1404.

Dixon, N., Spriggs, M. P., Smith, A., Meldrum, P. & Haslam, E. (2014). Quantification of reactivated landslide behaviour using acoustic emission monitoring. *Landslides* **1–12**, http://dx.doi.org/10.1007/s10346-014-0491-z.

Fujiwara, T., Ishibashi, A. & Monma, K. (1999). Application of acoustic emission method to Shirasu slope monitoring. In *Slope stability engineering* (Yagi, Yamagami & Jiang (eds)). Rotterdam: Balkema, pp. 147–150.

Garga, V. K. & Chichibu, A. (1990). A study of AE parameters and shear strength of sand. *Progress in Acoustic Emission V 10th Int. Acoustic Emission Symp., Sendai, Japan*, vol. **5**, 129–136.

Gunn, D. A., Chambers, J. E., Hobbs, P. R. N. *et al*. (2013). Rapid observations to guide the design of systems for long-term monitoring of a complex landslide in the Upper Lias Clays of North Yorkshire, UK. *Quart. J. Engng Geol. Hydrogeol*. **46**, No. 3, 323–336.

Hutchinson, J. N. (1988). General report: morphological and geotechnical parameters of landslides in relation to geology and hydrogeology. *Proc. 5th Int. Symp. on Landslides, Lausanne*, pp. 3–35.

Koerner, R. M., McCabe, M. W. & Lord, A. E. (1981). Acoustic emission behaviour and monitoring of soils. In *Acoustic emissions in geotechnical engineering practice*. West Conshohoken, PA: ASTM International, STP 750, pp. 93–141.

Leroueil, S. (2001). Natural slopes and cuts: movement and failure mechanisms. *Géotechnique* **51**, No. 3, 197–243.

Lord, A. E. & Koerner, R. M. (1974). Acoustic emission response of dry soils. *Test. Eval*. **2**, No. 3, 159–162.

Merritt, A. J., Chambers, J. E., Murphy, W. *et al*. (2013). 3D ground model development for an active landslide in Lias Mudrocks using geophysical, remote sensing and geotechnical methods. *Landslides* **11**, No. 4, 537–550.

Michlmayr, G., Cohen, D. & Or, D. (2012a). Sources and characteristics of acoustic emissions from mechanically stressed geologic granular media – a review. *Earth Sci. Rev*. **112**, No. 3, 97–114.

Michlmayr, G., Or, D. & Cohen, D. (2012b). Fiber bundle models for stress release and energy bursts during granular shearing. *Phys. Rev*. **86**, No. 061307, 1–7.

Michlmayr, G., Cohen, D. & Or, D. (2013). Shear-induced force fluctuations and acoustic emissions in granular material. *J. Geophys. Res.: Solid Earth* **118**, No. 12, 6086–6098.

Mitchell, R. J. & Romeril, P. M. (1984). Acoustic emission distress monitoring in sensitive clay. *Can. Geotech. J.* **21**, No. 1, 176–180.

Naemura, S., Tanaka, M., Nishikawa, S. *et al*. (1990). Acoustic emission of penetration experiments to judge soil condition. *J. Acoust. Emiss*. **10**, No. 1–2, 55–58.

Nakajima, I., Negishi, M., Ujihira, M. & Tanabe, T. (1991). Application of the acoustic emission monitoring rod to landslide measurement. *Proc. 5th Conf. on Acoustic Emission/Microseismic Activity in Geologic Structures and Materials, Pennsylvania*, pp. 1–15.

Rouse, C., Styles, P. & Wilson, S. A. (1991). Microseismic emissions from flowslide-type movements in South Wales. *Engng Geol*. **31**, No. 1, 91–110.

Schuster, R. L. & Krizek, R. J. (eds) (1978). *Landslides analysis and control*. Washington, DC: Transportation Research Board, Special report 176.

Shiotani, T. & Ohtsu, M. (1999). Prediction of slope failure based on AE activity. In *Acoustic emission: standards and technology update*. West Conshohoken, PA: ASTM International, STP 1353, pp. 156–172.